Research Square

Preprints are preliminary reports that have not undergone peer review.
They should not be considered conclusive, used to inform clinical practice,
or referenced by the media as validated information.

Comparative Diagnostic Accuracy of AI-Enhanced Mobile Limb-Lead ECG versus Cardiologist-Interpreted Standard 12-Lead ECG for Acute Myocardial Infarction

Yangyoun Lee
Ajou University School of Medicine
Young Hoon Ji
VUNO Inc
Yeongyeon Na
VUNO Inc
Hyun Jin Ahn
VUNO Inc
Sunghoon Joo
VUNO Inc
Mineok Chang
AIMS Bioscience Inc
Seok Oh
Chonnam National University Hospital, Chonnam National University Medical School
Yongwhan Lim
Chonnam National University Hospital, Chonnam National University Medical School
Dae Young Hyun
Chonnam National University Hospital, Chonnam National University Medical School
Min Chul Kim
VUNO Inc
Ki Hong Lee
Chonnam National University Hospital, Chonnam National University Medical School
Doo Sun Sim
Chonnam National University Hospital, Chonnam National University Medical School
Young Joon Hong
Chonnam National University Hospital, Chonnam National University Medical School
Ju Han Kim
Chonnam National University Hospital, Chonnam National University Medical School
Youngkeun Ahn
Chonnam National University Hospital, Chonnam National University Medical School

Moon-Seung Soh
Ajou University School of Medicine
Kyung Hoon Cho
zarazoro@hanmail.net

Chonnam National University Hospital, Chonnam National University Medical School

Research Article

Keywords: Myocardial infarction, Artificial intelligence, Electrocardiography, Mobile device, Diagnostic accuracy

Posted Date: November 10th, 2026

DOI: https://doi.org/10.21203/rs.3.rs-11476883/v1

License: This work is licensed under a Creative Commons Attribution 4.0 International License.
Read Full License

Additional Declarations: Competing interest reported. YHJ, YN, HJA, and SJ are employees of VUNO Inc. MC was an employee of VUNO Inc. The other authors declare that they have no competing interests.

Comparative Diagnostic Accuracy of AI-Enhanced Mobile Limb-Lead ECG versus Cardiologist-Interpreted Standard 12-Lead ECG for Acute Myocardial Infarction

Yangyoun Lee, MD,[1] Young Hoon Ji, MS,[2] Yeongyeon Na, MS,[2] Hyun Jin Ahn, MD,[2] Sunghoon Joo, PhD,[2] Mineok Chang, MD, PhD,[3] Seok Oh, MD, PhD,[4] Yongwhan Lim, MD,[4] Dae Young Hyun, MD,[4] Min Chul Kim, MD, PhD,[4] Ki Hong Lee, MD, PhD,[4] Doo Sun Sim, MD, PhD,[4] Young Joon Hong, MD, PhD,[4] Ju Han Kim, MD, PhD,[4] Youngkeun Ahn, MD, PhD,[4] Moon-Seung Soh, MD,[1*] and Kyung Hoon Cho, MD, PhD[4*]

Yangyoun Lee and Young Hoon Ji contributed equally to this study as first co-authors.

[1]Department of Cardiology, Ajou University School of Medicine, Suwon, Gyeonggi-do, Republic of Korea

[2]VUNO Inc., Seoul, Republic of Korea

[3]Section of Interventional Cardiology, MedStar Washington Hospital Center, Washington DC, USA

[4]Department of Cardiology, Chonnam National University Hospital, Chonnam National University Medical School, Gwangju, Republic of Korea

[*]Correspondence: Kyung Hoon Cho, MD, PhD, Department of Cardiology, Chonnam National University Medical School, 42 Jebong-ro, Dong-gu, Gwangju 61469, Republic of Korea. E-mail: zarazoro@hanmail.net; Tel: +82-62-220-6243; Fax: +82-62-228-7174

[*]Correspondence: Moon-Seung Soh, MD, Department of Cardiology, Ajou University School of Medicine, 164 World cup-ro, Yeongtong-gu, Suwon-si, Gyeonggi-do, Republic of Korea. E-mail: mssoh@hanmail.net; Tel: +82-31-219-5712; Fax: +82-31-219-4887

Abstract

Background: Deep learning models developed on standard 12-lead electrocardiograms (ECGs) can detect acute myocardial infarction (AMI), but their performance on limb-lead ECGs from mobile devices is uncertain. We evaluated an artificial intelligence (AI) model applied to mobile limb-lead ECGs for AMI detection, using cardiologist interpretation of truncated limb-lead and 12-lead ECGs as comparators.

Methods: We performed an analysis of a prospective observational cohort of 153 patients referred for coronary angiography at a Korean tertiary center (September 2022–October 2023). Each patient underwent mobile limb-lead and standard 12-lead ECG acquisition before revascularization. The model was applied without retraining to the mobile ECGs at two thresholds prespecified during model development (high sensitivity, high specificity), and three cardiologists independently interpreted truncated limb-lead and 12-lead ECGs. AMI was diagnosed according to the Fourth Universal Definition of Myocardial Infarction, with coronary angiography in all patients.

Results: Twenty-five patients (16.3%) had AMI, including 3 ST-elevation and 22 non-ST-elevation myocardial infarctions. The model achieved an area under the receiver operating characteristic curve of 0.843 (95% confidence interval, 0.758–0.928). At the high-sensitivity threshold, the model showed higher sensitivity than cardiologists interpreting truncated limb-lead and standard 12-lead ECGs (88.0% vs. 20.0% and 40.0%; both $p < 0.001$) and numerically higher negative predictive value (NPV; 95.9% vs. 85.5% and 88.6%), but lower specificity (55.5% vs. 92.2% and 91.4%; both $p < 0.001$) and positive predictive value (PPV; 27.8% vs. 33.3% and 47.6%). At the high-specificity threshold, specificity was similar to that of cardiologists interpreting standard 12-lead ECGs (93.8% vs. 91.4%; $p = 0.58$), and sensitivity did not differ significantly (48.0% vs. 40.0%; $p = 0.77$).

Conclusions: In this cohort, an AI-ECG model developed on standard ECGs discriminated AMI when applied to mobile limb-lead ECGs without retraining. At the high-sensitivity threshold, it showed higher sensitivity and numerically higher NPV but lower specificity and PPV than cardiologists' ECG interpretation. These findings support its potential as an adjunctive screening aid where 12-lead ECG acquisition or expert interpretation is delayed or unavailable.

Keywords: Myocardial infarction, Artificial intelligence, Electrocardiography, Mobile device, Diagnostic accuracy

Background

Ischemic heart disease remains a leading cause of global mortality, accounting for approximately 9 million deaths annually, with acute myocardial infarction (AMI) contributing substantially to this burden [1, 2]. As a time-critical medical emergency, AMI requires rapid and accurate diagnosis to enable timely intervention, thereby minimizing myocardial injury and reducing mortality [3, 4]. The Electrocardiogram (ECG) plays a central role in the diagnosis of AMI, guiding immediate clinical decision-making, including referral for primary percutaneous coronary intervention or further diagnostic evaluation, such as cardiac biomarker testing [3]. However, accurate electrocardiographic diagnosis remains challenging, because the manifestations of AMI vary according to the location and severity of myocardial injury.

Although ST-elevation myocardial infarction (STEMI) typically presents with overt findings such as ST-segment elevation, non-ST-elevation myocardial infarction (NSTEMI) often exhibits subtle or nonspecific ECG abnormalities, making accurate diagnosis more difficult [5]. These subtle features can hinder reliable interpretation even among experienced clinicians, contributing to inter-observer variability [6]. This difficulty may be further compounded when only reduced-lead ECG recordings are available. Although the standard

12-lead ECG remains the conventional ECG modality for evaluating suspected AMI, its acquisition requires dedicated equipment and trained personnel. Mobile single- or limb-lead devices have emerged as point-of-care tools that enable more rapid and convenient ECG acquisition. However, these recordings omit the precordial leads and therefore provide a more restricted view of the myocardium, which may further limit the detection of subtle ischemic changes.

Artificial intelligence (AI) may help address these limitations. Deep learning models have been reported to extract diagnostic information from the ECG signal that may not be readily apparent to human readers, potentially reducing inter-observer variability and identifying clinically relevant patterns from reduced-lead recordings. Recent advances in AI and mobile ECG technologies have demonstrated promising results in the detection of various cardiac conditions [7–12]. However, most AI-ECG models for AMI have been developed and validated on standard 12-lead recordings, and models for reduced-lead ECGs have generally been evaluated on leads extracted or reconstructed from standard recordings rather than on recordings acquired with a separate device [13–16]. Because acquisition hardware, electrode positions, posture, and signal quality differ between devices, whether a model developed on standard ECGs retains its diagnostic performance on recordings from a mobile device needs to be verified before such devices are used for AMI detection however evidence on this question remains limited.

To address this gap, we evaluated, in a prospective cohort of patients referred for coronary angiography, whether DeepECG-AMI, a deep learning model developed on standard ECGs [8], maintained its diagnostic performance for AMI when applied without retraining to limb-lead ECGs acquired with a mobile device, using cardiologists' interpretation of truncated limb-lead and standard 12-lead ECGs as comparators. As an exploratory secondary analysis,

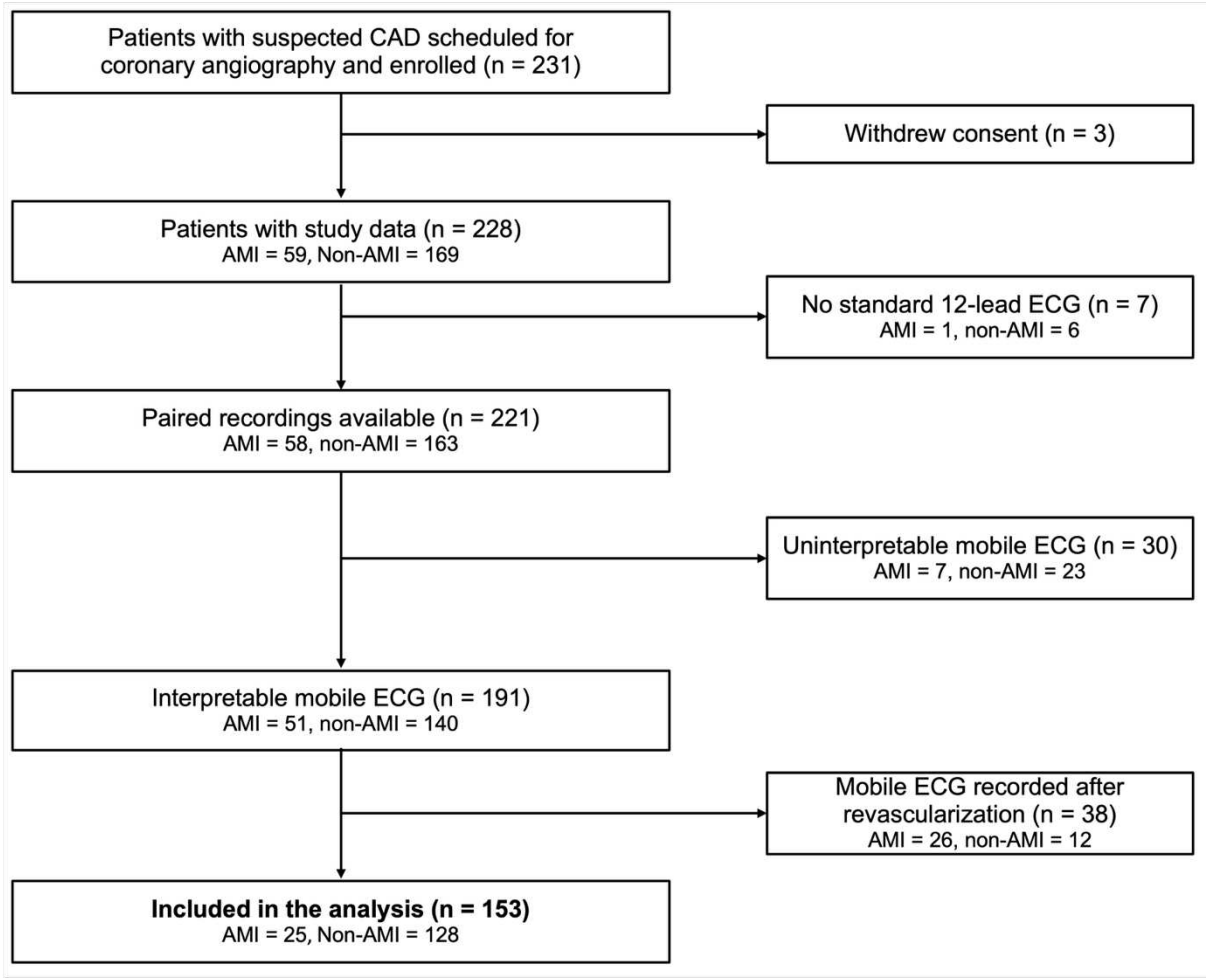
we evaluated whether the model-derived AMI probability could categorize patients into strata with differing AMI prevalence, without implying validated rule-in or rule-out thresholds.

Methods

Study design and patient enrollment

This diagnostic accuracy analysis used data from a prospective observational study conducted at Chonnam National University Hospital that included adult patients (aged ≥19 years) with a clinical suspicion of coronary artery disease (CAD) who were scheduled to undergo coronary angiography (CAG) between September 2022 and October 2023. Clinical suspicion of CAD was determined through standard clinical evaluation in the emergency department or outpatient setting, including medical history, electrocardiography, cardiac biomarker testing, and clinically indicated non-invasive functional or imaging studies. This study was approved by the Chonnam National University Hospital Institutional Review Board (CNUH-2022-375). The study was not registered, and this diagnostic accuracy analysis was not prespecified in the protocol but was conducted post hoc (Supplementary Material 1). The study is reported in compliance with the TRIPOD+AI reporting guideline [17] (Supplementary Material 2). Patients were enrolled consecutively from individuals presenting to the Department of Cardiology at the study hospital. Patients who were unable to use a mobile ECG device due to physical disabilities, as well as those with pacemakers, implantable cardioverter-defibrillators, ventricular assist devices, or other intracardiac devices, were excluded from the study. (Fig. 1)

Fig. 1 Flow of participants through the study.



Numbers of patients with and without acute myocardial infarction (AMI) are shown at each step. AMI, acute myocardial infarction; CAD, coronary artery disease; ECG, electrocardiogram.

Definition of AMI and clinical criteria

In this study, AMI and its subtypes were defined according to the Fourth Universal Definition of Myocardial Infarction [18]. For this analysis, AMI included both type 1 and type 2 myocardial infarction, whereas non-ischemic myocardial injury was classified as non-AMI. AMI was further classified as STEMI or NSTEMI based on electrocardiographic criteria from current guidelines [19]. The final diagnosis of AMI was established through a comprehensive assessment of cardiac biomarkers, standard 12-lead ECG results, CAG findings, and clinical evaluation. All patients underwent CAG.

Data acquisition and ECG pairing

Each patient underwent both a mobile limb-lead ECG using the mobile ECG device (HATIV® P30, VUNO Inc., Seoul, Republic of Korea) and a standard 12-lead ECG acquired using the MUSE system (GE HealthCare, Chicago, IL, USA). ECG acquisition was performed either before or after CAG. Mobile limb-lead ECGs were recorded with patients in a sitting position for 30 seconds using a handheld mobile device equipped with three electrodes, two positioned on the front surface and one on the back surface (Fig. 2a). From each recording, a 10-second segment with interpretable signal quality was selected from the central portion for analysis. Standard 12-lead ECGs were obtained as part of the routine diagnostic workup. For each patient, the mobile limb-lead ECG was paired with the temporally closest standard 12-lead ECG. Mobile ECG recordings obtained after revascularization were excluded, and only ECG pairs acquired before revascularization were analyzed.

Demographic, clinical, laboratory, and echocardiographic variables were collected (Table 1). Some variables contained missing values because the corresponding tests were not performed in all patients as part of routine clinical care.

Table 1 Baseline characteristics of study participants according to the presence of acute myocardial infarction

	Total (N = 153)	Non-AMI (N = 128, 83.7%)	AMI (N = 25, 16.3%)	p-value
Age, years	64.9 ± 9.8	64.5 ± 9.7	67.0 ± 10.1	0.233
Female	41 (26.8%)	34 (26.6%)	7 (28.0%)	1.000
Height, cm	164.3 ± 8.1	164.4 ± 8.4	163.6 ± 6.1	0.671
Weight, kg	67.5 ± 10.6	67.7 ± 10.9	66.6 ± 9.0	0.641
Body mass index, kg/m^2	25.0 ± 2.9	25.0 ± 2.9	24.8 ± 2.7	0.820
Hypertension	72 (47.1%)	57 (44.5%)	15 (60.0%)	0.231
Diabetes mellitus	50 (32.7%)	40 (31.2%)	10 (40.0%)	0.535
Creatinine level, mg/dL, median (IQR)	0.86 (0.72–0.97)	0.86 (0.73–0.97)	0.81 (0.70–0.94)	0.615
Potassium level, mEq/L	4.1 ± 0.3	4.1 ± 0.3	4.2 ± 0.4	0.179
Hemoglobin, g/dL	13.2 ± 1.6	13.4 ± 1.6	12.4 ± 1.9	0.005
Platelet count, ×10^3/μL	202.9 ± 50.8	200.5 ± 49.3	215.4 ± 57.1	0.178
Troponin I, ng/mL, median (IQR)	0.01 (0.00–0.03) (NA 18)	0.01 (0.00–0.01) (NA 18)	0.29 (0.10–1.18)	<0.001

	Total (N = 153)	Non-AMI (N = 128, 83.7%)	AMI (N = 25, 16.3%)	p-value
Left ventricular ejection fraction, %	64.2 ± 10.2 (NA 26)	65.9 ± 8.3 (NA 24)	56.3 ± 13.8 (NA 2)	<0.001
ACS type				
STEMI	3 (2.0%)	0 (0.0%)	3 (12.0%)	–
NSTEMI	22 (14.4%)	0 (0.0%)	22 (88.0%)	–
Unstable angina	85 (55.6%)	85 (66.4%)	0 (0.0%)	–
Revascularization				
PCI	38 (24.8%)	24 (18.8%)	14 (56.0%)	<0.001
CABG	1 (0.7%)	0 (0.0%)	1 (4.0%)	0.163
Target vessels				
Left anterior descending artery	27 (17.6%)	18 (14.1%)	9 (36.0%)	0.018
Left circumflex artery	16 (10.5%)	9 (7.0%)	7 (28.0%)	0.006
Right coronary artery	12 (7.8%)	9 (7.0%)	3 (12.0%)	0.416
Multiple vessels	9 (5.9%)	4 (3.1%)	5 (20.0%)	0.006
Electrocardiographic characteristics				
Atrial fibrillation	4 (2.6%)	4 (3.1%)	0 (0.0%)	1.000
Heart rate, bpm	64.2 ± 10.2	62.9 ± 9.4	71.0 ± 11.4	<0.001
PR interval, ms	178.1 ± 26.1 (NA 6)	178.2 ± 24.7 (NA 6)	177.8 ± 32.5	0.944
QRS duration, ms	97.1 ± 15.9	97.1 ± 16.1	97.4 ± 15.0	0.932
QT interval, ms	418.7 ± 30.6	418.3 ± 30.7	420.6 ± 31.0	0.724
QT corrected, ms	429.6 ± 29.8	424.8 ± 24.8	454.2 ± 40.0	<0.001

Data are presented as mean ± standard deviation, median (interquartile range), or number (percentage). Continuous variables were compared using Student's t-test or the Mann-Whitney U test, and categorical variables using Pearson's chi-square test or Fisher's exact test when any expected cell count was <5. Missing values are indicated by 'NA' in the table. Electrocardiographic characteristics were derived from 12-lead numeric values computed by the MUSE system. QT corrected interval is a heart rate-adjusted value.

Abbreviations: ACS, acute coronary syndrome; AMI, acute myocardial infarction; CABG, coronary artery bypass grafting; IQR, interquartile range; NSTEMI, non-ST-elevation myocardial infarction; PCI, percutaneous coronary intervention; STEMI, ST-elevation myocardial infarction.

Performance comparison protocol: AI model versus cardiologist interpretation

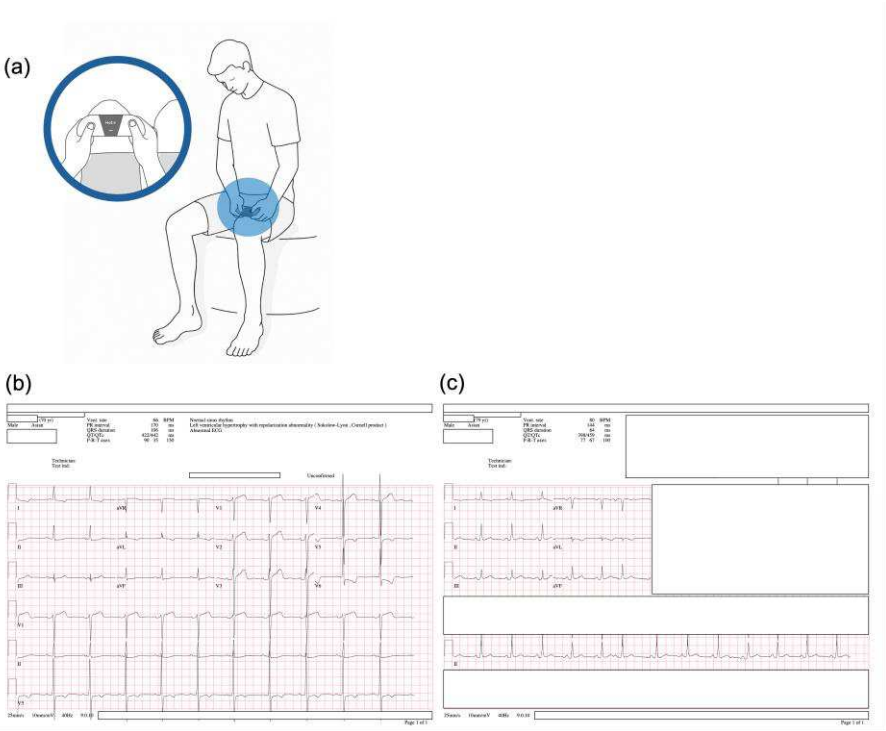
Diagnostic accuracy was compared across three approaches: (1) the AI model on mobile limb-lead ECGs, (2) cardiologist interpretation of truncated limb-lead ECGs, and (3) cardiologist interpretation of standard 12-lead ECGs.

The AI model, DeepECG-AMI [8], was previously developed to detect AMI using multiple lead configurations, including 12-lead, limb-lead, and lead I ECGs (Supplementary Material 3: Supplementary Methods 1). In the present study, the model was applied to mobile limb-lead ECGs without retraining. Two operating thresholds were prespecified during model development: one optimized for Youden's J statistic (the high-sensitivity threshold) and the other for the F1-score (the high-specificity threshold). Unless otherwise specified, the

threshold maximizing Youden's J was used (Supplementary Material 3: Supplementary Methods 2). The model analyzed ECG signals exclusively and did not incorporate demographic or clinical information.

Truncated limb-lead ECGs were generated from the standard 12-lead recordings by masking the six precordial leads (V1–V6) and removing the machine-generated interpretation, leaving the limb leads with ECG numeric values (Fig. 2b, c). For interpretation of these tracings, cardiologists were provided with basic patient information, including age, sex, ECG numeric values, and the overall AMI prevalence in the study cohort, to reflect real-world clinical settings. For interpretation of 12-lead ECGs, cardiologists additionally reviewed automated ECG interpretations generated by the MUSE system, as provided in routine clinical practice. Cardiologists classified each ECG as AMI or non-AMI.

Fig. 2 Acquisition of mobile limb-lead electrocardiogram and example of standard and truncated limb-lead electrocardiograms used in cardiologist interpretation.



(a) Mobile limb-lead ECG was recorded using a mobile device equipped with three electrodes, two positioned on the front and one on the back. (b) Standard 12-lead ECG including limb and precordial leads with machine-generated interpretation. (c) Truncated limb-lead ECG derived by masking the precordial leads (V1–V6) from the 12-lead ECG, with machine-generated interpretation removed. ECG, electrocardiogram.

All ECGs were independently interpreted by three board-certified cardiologists from separate institutions, none of whom were affiliated with the data-collecting hospital. To minimize recall bias, a washout period of approximately 1 month separated the interpretation sessions for truncated limb-lead ECGs and standard 12-lead ECGs. For the cardiologist comparator, a positive ECG interpretation for AMI was assigned when at least two of the three cardiologists classified the ECG as AMI.

Subgroup, sensitivity, and exploratory probability stratification analyses

Subgroup analyses were performed to compare diagnostic accuracy across age groups (≥65 years vs. <65 years) and sex (male vs. female). Additional analyses compared the sensitivity for detecting NSTEMI between the AI model and cardiologists' interpretations using truncated limb-lead ECGs and standard 12-lead ECGs. To assess the robustness of diagnostic performance to differences in acquisition timing between mobile and standard ECGs, sensitivity analyses were performed using ECG pairs obtained within 3, 6, 12, and 24 hours of each other.

For exploratory evaluation of the model's probability output beyond binary classification, patients were categorized into three strata using the two operating thresholds (Youden's J and F1) described above (Supplementary Material 3: Supplementary Methods 2): a low-probability stratum below the lower threshold (Youden's J), a high-probability stratum above the upper threshold (F1), and an intermediate stratum between the two thresholds.

Statistical analysis

Continuous variables were summarized as mean ± standard deviation or median (interquartile range) based on distribution normality and were compared using Student's t-test or the Mann-Whitney U test. Categorical variables were summarized as frequencies (percentages) and compared using Pearson's chi-square test, or Fisher's exact test when any expected cell count was <5.

Diagnostic performance was assessed by sensitivity, specificity, positive predictive value (PPV), negative predictive value (NPV), positive and negative likelihood ratios (LR+, LR−), and, for the AI model only, the area under the receiver operating characteristic curve (AUROC). Ninety-five percent confidence intervals (CIs) were calculated using the DeLong method for AUROC [20], the Wilson score method for proportions [21], and the Simel–Samsa–Matchar log-transformation for likelihood ratios [22]. Between-method comparisons preserved within-patient pairing: sensitivity and specificity were compared using McNemar's exact test. PPV and NPV were not formally compared, as they depend on disease prevalence; LR+ and LR− follow directly from sensitivity and specificity. Stratum-level prevalence and interval likelihood ratios were reported with 95% CIs.

Model calibration was assessed descriptively [23, 24], including calibration-in-the-large and calibration slope (via logistic recalibration; 95% CIs from bias-corrected and accelerated [BCa] bootstrap, B = 2,000) [25]. Overall prediction error was assessed using the Brier score, referenced against a null model assigning the overall observed AMI prevalence (16.3%) to every patient. Observed AMI proportions by predicted-probability quintile were plotted with 95% Wilson CIs alongside a restricted cubic spline calibration curve [26]. Given the limited number of AMI events, calibration was interpreted without formal hypothesis testing.

Inter-reader agreement among the three cardiologists was assessed using Fleiss' κ [27] and pairwise Cohen's κ [28] with 95% CIs from BCa bootstrap resampling (B = 2,000) [25]. The majority-vote cardiologist interpretation was used as the comparator against the AI model in the primary analysis, and reader-level diagnostic performance metrics and agreement statistics were reported in Supplementary Material 3: Table S1 and Table S2.

A two-sided p-value of <0.05 was considered statistically significant. Statistical analyses were conducted using Python (version 3.11.7) and R (version 4.4.3; R Core Team), with

relevant packages used for data analysis. Claude (Anthropic) was used to assist with code development and manuscript editing.

Results

Participants and baseline characteristics

Of the 231 enrolled patients, 3 withdrew consent, 7 had no standard 12-lead ECG, and 30 had uninterpretable mobile recordings due to electrode misplacement or acquisition artifacts (unreadable signal, n = 25; limb-lead reversal, n = 5), resulting in 191 patients, including 51 with AMI. Of the 51 patients with AMI, 11 had STEMI, of whom 8 were excluded because their mobile ECGs were recorded after revascularization. Consequently, 153 patients (25 with AMI) were included in the final analysis (Fig. 1). Details of the sample size determination are provided in Supplementary Material 1.

The final cohort comprised 153 patients with paired mobile limb-lead and standard 12-lead ECGs (mean age 64.9 ± 9.8 years; 41 [26.8%] female). Twenty-five patients (16.3%) were diagnosed with AMI, including 3 with STEMI and 22 with NSTEMI, whereas 128 (83.7%) were classified as non-AMI. The non-AMI group included patients with unstable angina (n = 85) and other ischemic or structural heart diseases, reflecting the clinically selected population referred for coronary angiography. Revascularization was performed in 15 patients with AMI (60.0%) and 24 without AMI (18.8%). Compared with those without AMI, patients with AMI had lower hemoglobin and left ventricular ejection fraction and higher heart rate and corrected QT interval ($p = 0.005$ for hemoglobin and $p < 0.001$ for the others), whereas age, sex, hypertension, and diabetes did not differ significantly (Table 1).

Diagnostic performance comparison between the AI model and cardiologists

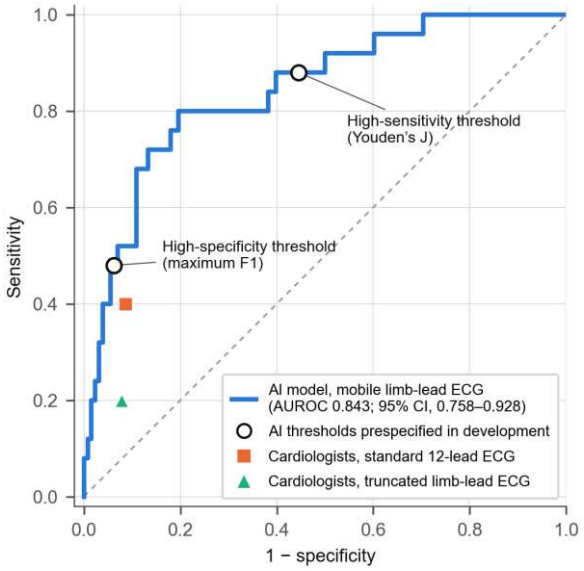
The AUROC of the AI model was 0.843 (95% CI, 0.758–0.928) (Fig. 3). At the high-sensitivity threshold, sensitivity was higher than that of the cardiologists' 12-lead

interpretation (88.0% vs. 40.0%; difference, 48.0 percentage points; 95% CI, 24.1 to 65.1) and specificity was lower (55.5% vs. 91.4%; difference, −35.9 percentage points; 95% CI, −44.6 to −26.6; both $p < 0.001$) (Table 2). At an AMI prevalence of 16.3%, the PPV and NPV were 27.8% and 95.9%, compared with 47.6% and 88.6% for the cardiologists' 12-lead interpretation. Compared with the cardiologists' interpretation of the truncated limb-lead ECGs (sensitivity 20.0%, specificity 92.2%), sensitivity was also higher at this threshold (88.0% vs. 20.0%), with lower specificity (55.5% vs. 92.2%; both $p < 0.001$).

At the high-specificity threshold, sensitivity did not differ significantly from that of the cardiologists' 12-lead interpretation (48.0% vs. 40.0%; difference, 8.0 percentage points; 95% CI, −18.3 to 32.9; $p = 0.77$), and specificity was similar (93.8% vs. 91.4%; difference, 2.3 percentage points; 95% CI, −3.7 to 8.6; $p = 0.58$). The PPV and NPV were 60.0% and 90.2%, respectively. Compared with the cardiologists' interpretation of the truncated limb-lead ECGs, sensitivity was numerically higher at a similar specificity (difference, 28.0 percentage points; 95% CI, 0.7 to 50.3; $p = 0.09$).

For NSTEMI ($n = 22$), the AI model detected 19 of 22 cases at the high-sensitivity threshold (sensitivity 86.4%; 95% CI, 66.7–95.3%), compared with 3 of 22 by cardiologists using truncated limb-lead ECGs (13.6%; 95% CI, 4.7–33.3%; $p < 0.001$) and 8 of 22 using standard 12-lead ECGs (36.4%; 95% CI, 19.7–57.0%; $p < 0.001$).

Fig. 3 Diagnostic performance of the AI model for detecting acute myocardial infarction (AMI).



Receiver operating characteristic curve for the AI model applied to mobile limb-lead ECGs, with the two thresholds prespecified during model development (open circles) and the majority-vote cardiologist operating points for standard 12-lead ECGs (square) and truncated limb-lead ECGs (triangle). AI, artificial intelligence; AUROC, area under the receiver operating characteristic curve; CI, confidence interval; ECG, electrocardiogram.

Table 2 Diagnostic performance of the AI model and cardiologists for acute myocardial infarction

	AI model, high-sensitivity threshold	AI model, high-specificity threshold	Cardiologists, standard 12-lead ECG	Cardiologists, truncated limb-lead ECG
Threshold	0.1422	0.2671	–	–
TP/FP/FN/TN	22/57/3/71	12/8/13/120	10/11/15/117	5/10/20/118
Sensitivity, % (95% CI)	88.0 (70.0–95.8)	48.0 (30.0–66.5)	40.0 (23.4–59.3)	20.0 (8.9–39.1)
p-value*	–	–	<0.001 / 0.774	<0.001 / 0.092
Specificity, % (95% CI)	55.5 (46.8–63.8)	93.8 (88.2–96.8)	91.4 (85.3–95.1)	92.2 (86.2–95.7)
p-value*	–	–	<0.001 / 0.581	<0.001 / 0.804
PPV, % (95% CI)	27.8 (19.2–38.6)	60.0 (38.7–78.1)	47.6 (28.3–67.6)	33.3 (15.2–58.3)
NPV, % (95% CI)	95.9 (88.7–98.6)	90.2 (84.0–94.2)	88.6 (82.1–93.0)	85.5 (78.7–90.4)
LR+ (95% CI)	1.98 (1.55–2.52)	7.68 (3.50–16.84)	4.65 (2.22–9.77)	2.56 (0.96–6.85)
LR− (95% CI)	0.22 (0.07–0.63)	0.55 (0.38–0.81)	0.66 (0.47–0.91)	0.87 (0.71–1.06)

The AI model was applied to mobile limb-lead ECGs (n = 153; 25 with AMI) at two thresholds prespecified during model development using the internal validation cohort: the high-sensitivity threshold (0.1422), selected by maximizing Youden's J statistic, and the high-specificity threshold (0.2671), selected by maximizing the F1-score; the AUROC of the AI model was 0.843 (0.758–0.928). Cardiologists interpreted truncated limb-lead and standard 12-lead ECGs, and their results were based on majority voting by three readers. Sensitivity, specificity, PPV, and NPV are presented with 95% CIs; LR+ and LR− were calculated from sensitivity and specificity. *p-values compare each cardiologist reading with the AI model at the high-sensitivity / high-specificity threshold, respectively, and were calculated using the exact McNemar test.

Abbreviations: AI, artificial intelligence; AMI, acute myocardial infarction; AUROC, area under the receiver operating characteristic curve; CI, confidence interval; ECG, electrocardiogram; FN, false negative; FP, false

positive; LR, likelihood ratio; NPV, negative predictive value; PPV, positive predictive value; TN, true negative; TP, true positive.

Inter-reader agreement

Agreement among the three cardiologists was higher for standard 12-lead than for truncated limb-lead interpretation: Fleiss' κ was 0.40 (95% CI, 0.29–0.53) versus 0.27 (95% CI, 0.14–0.44), and pairwise Cohen's κ ranged from 0.31 to 0.52 versus 0.22 to 0.34. Reader-level diagnostic performance and inter-reader agreement statistics are provided in Supplementary Material 3: Table S1 and Table S2.

Table 3 Exploratory subgroup analysis of AI model performance by age and sex

	Age		Sex	
	<65 years, N = 71	**≥65 years, N = 82**	**Male, N = 112**	**Female, N = 41**
AMI, n (%)	8 (11.3%)	17 (20.7%)	18 (16.1%)	7 (17.1%)
Sensitivity, % (95% CI)	100.0 (67.6–100.0)	82.4 (59.0–93.8)	94.4 (74.2–99.0)	71.4 (35.9–91.8)
Specificity, % (95% CI)	55.6 (43.3–67.2)	55.4 (43.3–66.8)	59.6 (49.5–68.9)	44.1 (28.9–60.5)
PPV, % (95% CI)	22.2 (11.7–38.1)	32.6 (20.5–47.5)	30.9 (20.3–44.0)	20.8 (9.2–40.5)
NPV, % (95% CI)	100.0 (90.1–100.0)	92.3 (79.7–97.3)	98.2 (90.7–99.7)	88.2 (65.7–96.7)

The AI model was evaluated using mobile limb-lead ECGs at the prespecified Youden's J threshold from the internal validation cohort. Values are presented as percentages with 95% CIs in parentheses. Subgroup analyses were exploratory and interpreted descriptively; no formal between-subgroup hypothesis testing was performed. Abbreviations: AI, artificial intelligence; AMI, acute myocardial infarction; CI, confidence interval; NPV, negative predictive value; PPV, positive predictive value

Subgroup and sensitivity analyses

Performance was examined across age and sex subgroups (Table 3). Estimates were broadly similar between patients younger than 65 years and those aged 65 years or older (sensitivity 100.0% vs. 82.4%), with overlapping confidence intervals across all metrics. Performance estimates were numerically lower in female than in male patients (sensitivity 71.4% vs. 94.4%; specificity 44.1% [95% CI, 28.9–60.5%] vs. 59.6% [95% CI, 49.5–68.9%]), but confidence intervals overlapped and the female subgroup was small. NPV was 88.2% or higher in all subgroups. Because event counts within subgroups were limited, these analyses were exploratory and were not formally tested for between-subgroup differences.

When the analysis was restricted to ECG pairs recorded within 3, 6, 12, or 24 hours of each other (n = 40 to 143; 8 to 18 with AMI), the AUROC ranged from 0.848 to 0.912 (Table 4). At the high-sensitivity threshold, sensitivity ranged from 87.5% to 92.9% with specificity of 53.1% to 58.3%, compared with 37.5% to 50.0% sensitivity and 90.6% to 93.1% specificity for the cardiologists' 12-lead interpretation. At the high-specificity threshold, sensitivity ranged from 61.1% to 72.7% with specificity of 90.6% to 94.4%.

Table 4 Sensitivity analyses of AI model performance compared with cardiologists' 12-lead interpretation

Analysis	n (AMI)	AUROC (95% CI)	High-sensitivity threshold, Se / Sp, %	High-specificity threshold, Se / Sp, %	Cardiologists, 12-lead, Se / Sp, %
Main analysis	153 (25)	0.843 (0.758–0.928)	88.0 / 55.5	48.0 / 93.8	40.0 / 91.4
Interval between mobile and standard ECGs					
≤3 h	40 (8)	0.848 (0.677–1.000)	87.5 / 53.1	62.5 / 90.6	37.5 / 90.6
≤6 h	83 (11)	0.904 (0.795–1.000)	90.9 / 58.3	72.7 / 94.4	45.5 / 93.1
≤12 h	116 (14)	0.912 (0.826–0.998)	92.9 / 55.9	71.4 / 94.1	50.0 / 91.2
≤24 h	143 (18)	0.863 (0.763–0.962)	88.9 / 56.8	61.1 / 93.6	44.4 / 91.2

Values are sensitivity / specificity (%). Pairs were restricted by the absolute interval between the mobile and standard ECG recordings. Cardiologists, majority interpretation of the standard 12-lead ECG.

Abbreviations: AI, artificial intelligence; AMI, acute myocardial infarction; AUROC, area under the receiver operating characteristic curve; CI, confidence interval; ECG, electrocardiogram; Se, sensitivity; Sp, specificity

Interval likelihood ratios across AI-defined AMI probability strata

AMI prevalence within strata and interval LRs differed across the three exploratory AI-defined probability strata (Table 5). AMI prevalence increased from 4.1% (95% CI, 1.4–11.3) in the low-probability stratum (n = 74; 48.4% of the cohort) to 16.9% (95% CI, 9.5–28.5) in the intermediate stratum (n = 59; 38.6%) and 60.0% (95% CI, 38.7–78.1) in the high-probability stratum (n = 20; 13.1%), with corresponding interval LRs of 0.22, 1.04, and 7.68.

Table 5 AMI prevalence within strata and interval likelihood ratios across AI-defined probability strata

AI probability stratum	n (%)	AMI / non-AMI	AMI prevalence within stratum, % (95% CI)	AMI cases by stratum, %	Non-AMI cases by stratum, %	Interval LR (95% CI)
High AI-probability[a]	20 (13.1)	12 / 8	60.0 (38.7–78.1)	48.0	6.2	7.68 (3.50–16.84)
Intermediate AI-probability[b]	59 (38.6)	10 / 49	16.9 (9.5–28.5)	40.0	38.3	1.04 (0.62–1.77)
Low AI-probability[c]	74 (48.4)	3 / 71	4.1 (1.4–11.3)	12.0	55.5	0.22 (0.07–0.63)
Total	*153 (100)*	*25 / 128*	*16.3 (11.3–22.9)*	*100*	*100*	–

Patients were categorized into three exploratory AI-defined probability strata using two prespecified operating thresholds derived from the internal validation cohort. The high-probability stratum was defined as patients above the upper threshold, the low-probability stratum as patients below the lower threshold, and the intermediate-probability stratum as patients between the two thresholds. Within-stratum AMI prevalence corresponds to *P*(AMI|stratum), whereas the distributions of AMI and non-AMI cases across strata correspond to *P*(stratum|AMI) and *P*(stratum|non-AMI), respectively. Interval likelihood ratios were calculated as *P*(stratum|AMI) / *P*(stratum|non-AMI). Within-stratum AMI prevalence 95% CIs were calculated using the Wilson score method, and interval LR 95% CIs were calculated using the Simel–Samsa–Matchar method. [a]Above the upper operating threshold selected by maximizing the F1-score. [b]Between the two operating thresholds. [c]Below the lower operating threshold selected by Youden's J statistic.

Abbreviations: AI, artificial intelligence; AMI, acute myocardial infarction; CI, confidence interval; LR, likelihood ratio

Model calibration

Calibration-in-the-large was −0.05 (95% CI, −0.47 to 0.38), the calibration slope was 2.40 (95% CI, 1.45–3.66), and the Brier score was 0.110 (null model, 0.137), indicating good mean calibration but a steeper observed risk gradient than predicted (slope >1). These calibration results are summarized in Supplementary Material 3: Fig. S1.

Discussion

In this prospective cohort of patients referred for coronary angiography, a deep learning model developed on standard ECGs discriminated AMI from mobile limb-lead recordings without retraining (AUROC, 0.843). At the prespecified high-sensitivity threshold, the model detected more AMI than cardiologists, most of which were NSTEMI, at the cost of more false positives; at the prespecified high-specificity threshold, whose specificity was close to that of cardiologists reading standard 12-lead ECGs, sensitivity did not differ significantly

from that of the cardiologists. The direction of these findings was unchanged when analyses were restricted to closely timed ECG pairs (Table 4).

Comparison with prior studies and clinical relevance

Previous studies have demonstrated the feasibility of AI-based AMI detection using standard 12-lead ECGs or reduced-lead approaches. For example, Cho et al. reported AUROCs of 0.880 and 0.854 and sensitivities of 80.0% and 72.0% in internal and external validation, respectively, for AMI detection using a variational autoencoder–based reconstruction model applied to six-lead ECGs derived from standard 12-lead recordings [13]. In the multicenter ROMIAE (Rule-Out acute Myocardial Infarction using Artificial intelligence Electrocardiogram analysis) study, Lee et al. reported a sensitivity of approximately 65.5% for NSTEMI detection, with high specificity, using a 12-lead ECG-based AI model in an emergency department setting [29].

A distinguishing feature of the present study is that the AI model was applied to ECGs acquired directly from a dedicated mobile limb-lead device, rather than to reduced-lead signals reconstructed or truncated from standard 12-lead recordings, as in several prior reports [14–16]. In addition, AMI was diagnosed according to the universal definition of myocardial infarction based on CAG findings, cardiac biomarkers, standard 12-lead ECG results, and clinical assessment, with CAG performed in all patients to support a clinically relevant reference standard. Direct comparison with prior studies is limited by differences in cohort spectrum, AMI prevalence, ECG acquisition modality, model architecture, operating thresholds, and reference standards. Accordingly, the higher sensitivity observed in the present study at the selected operating threshold should not be interpreted as evidence of superiority. Rather, our findings are broadly consistent with prior reports suggesting that AI-based ECG interpretation may improve sensitivity for AMI detection in selected settings,

whereas the accompanying lower specificity supports a screening-oriented rather than confirmatory role.

Differences between the model and the cardiologists were largest when only limb leads were available. The cardiologists' sensitivity was numerically higher with the precordial leads (40.0%) than on truncated limb-lead ECGs (20.0%), whereas at a similar specificity the model's sensitivity on mobile limb-lead ECGs was 48.0%, numerically higher than that of the cardiologists reading limb leads alone. This suggests that the model may use limb-lead information that is difficult for human readers to interpret.

Performance in detecting NSTEMI

The electrocardiographic changes of NSTEMI are often subtle and of limited diagnostic and localizing value; for example, in patients with single-vessel NSTEMI, Gifft et al. reported that the distribution of ischemic ECG changes identified the culprit vessel with a sensitivity of only 41.5% [30]. Consistent with these challenges, cardiologist interpretations in the present study showed low sensitivity for NSTEMI detection using both truncated limb-lead ECGs (13.6%) and standard 12-lead ECGs (36.4%). In contrast, the AI model applied to mobile limb-lead ECGs showed higher sensitivity at the high-sensitivity threshold, exceeding that of cardiologists even when they interpreted standard 12-lead ECGs with precordial leads. Notably, at the high-sensitivity threshold, the detection sets were nested: every AMI case identified by cardiologists on either modality was also identified by the model, with no case detected by readers but missed by the model (discordant pairs, model-positive/reader-negative versus reader-positive/model-negative, across all 25 AMI cases: 17/0 for truncated limb-lead and 12/0 for standard 12-lead ECGs; 16/0 and 11/0 when restricted to the 22 NSTEMI cases). The three cases missed by the model were all NSTEMI with probabilities below the threshold, and all three were classified as negative by all three cardiologists on both modalities; two involved the left circumflex artery, a territory in which infarction often

presents without ST-segment elevation and, in more than one-third of patients in one series, without significant ST-segment changes on the admission ECG [31, 32].

The model may capture subtle repolarization or morphological patterns not readily apparent to human readers. This finding is directionally consistent with prior reports of AI-enhanced NSTEMI detection, including the ROMIAE study [29], although absolute sensitivities are not directly comparable given differences in cohort, AMI prevalence, acquisition modality, model, and reference standard. The NSTEMI analysis was based on only 22 cases, with wide uncertainty requiring confirmation in larger cohorts. Within these limitations, the model's higher sensitivity for NSTEMI at the high-sensitivity threshold supports its potential role as a screening-oriented adjunct to reduce missed cases, rather than as a stand-alone diagnostic tool.

Exploratory probability stratification and potential clinical implications

Beyond binary classification, the model's continuous probability output enabled exploratory categorization of patients into low-, intermediate-, and high-probability strata. The high-probability stratum was enriched for AMI (interval LR 7.68), whereas the low-probability stratum showed a lower within-stratum AMI prevalence (interval LR 0.22). The intermediate stratum had an interval LR close to unity, indicating little change from the cohort pre-test probability, and comprised 38.6% of the cohort. These findings suggest that the model-derived probability provided risk stratification beyond a binary decision, identifying a subgroup enriched for AMI while leaving a sizable intermediate group in whom the output was less clinically informative.

However, these findings should be interpreted cautiously. Three AMI cases (12.0% of all AMI cases) were assigned to the low-probability stratum, so this stratum should not be interpreted as a safe rule-out category. Similarly, the high-probability stratum showed a within-stratum AMI prevalence of 60.0%, limiting its use as a stand-alone trigger for invasive

evaluation. Mobile ECG–based probability estimation may therefore be best viewed as a potential adjunct to conventional diagnostic pathways. Which threshold is appropriate depends on the intended use and cannot be determined from this study.

Acquisition differences between mobile and standard ECGs

The standard and mobile recordings differed in device, lead configuration, posture, and acquisition time. The timing also differed by AMI status: in patients with AMI, the mobile ECG was recorded a median of 6.8 hours after the standard 12-lead ECG, whereas in patients without AMI it preceded the standard ECG by a median of 2.3 hours. This could have favored the model if ischemic changes evolved between the recordings; however, the direction of the findings was unchanged when the analysis was restricted to closely timed pairs (Table 4).

Limitations

Several limitations should be acknowledged. First, this was a single-center study with a limited number of AMI events (3 STEMI and 22 NSTEMI). The small event count resulted in wide confidence intervals for between-method differences (for example, −18.3 to 32.9 percentage points for sensitivity at the high-specificity threshold), reduced the precision of subgroup, stratum-level, and calibration estimates, and precluded meaningful conclusions regarding STEMI; the findings should therefore be interpreted primarily in relation to NSTEMI detection. The scarcity of STEMI cases largely reflected the exclusion of recordings obtained after revascularization: of the 11 patients with STEMI who had interpretable paired recordings, 8 were excluded on this basis, consistent with the urgency of reperfusion in STEMI leaving little opportunity for research ECG acquisition beforehand. Second, patients were enrolled based on an indication for CAG, which may have introduce selection bias and limits generalizability to broader, unselected chest-pain, emergency department, or prehospital populations. Third, the raw probability outputs showed imperfect

calibration in this cohort: although calibration-in-the-large was near zero, the calibration slope was well above 1 (2.40), indicating under-dispersed predictions that overstated risk at lower and understated risk at higher predicted probabilities. This miscalibration may have been driven by the application of the model, which was not trained on mobile limb-lead ECGs, to a cohort that differed from its development cohort. Therefore, the probability strata should be regarded as exploratory and would require external validation and potential recalibration before any threshold-based clinical application. Fourth, handheld mobile ECG recordings may be more susceptible to acquisition-related variability than standard 12-lead ECGs, potentially affecting signal quality. Of 231 enrolled patients, 30 (13.0%) were excluded due to uninterpretable recordings caused by electrode misplacement or acquisition artifacts. Thus, the reported diagnostic performance may overestimate real-world performance. Furthermore, to avoid interfering with routine clinical care, the recordings were obtained at different times, with intervals differing between patients with and without AMI. As ischemic ECG findings may evolve over time, these temporal differences may have affected the comparability of the recordings. Finally, further prospective validation in real-world point-of-care, emergency, and prehospital settings is needed to determine clinical utility, workflow impact, and safety.

Conclusions

In patients referred for coronary angiography, DeepECG-AMI, developed on standard ECGs, discriminated AMI when applied without retraining to mobile limb-lead ECGs. At the prespecified high-sensitivity threshold, it detected more NSTEMI than cardiologists at the cost of more false positives, whereas at the prespecified high-specificity threshold, with a specificity similar to that of cardiologists interpreting standard 12-lead ECGs, its sensitivity did not differ significantly. These findings suggest a potential role as an adjunctive screening aid where standard 12-lead acquisition or expert interpretation is not immediately available.

Given the single-center design, limited number of AMI events, and exploratory nature of the analyses, prospective evaluation in larger, unselected cohorts of patients with suspected acute coronary syndrome, with device-specific recalibration, is warranted before clinical application.

Abbreviations

ACS: Acute coronary syndrome; AI: Artificial intelligence; AMI: Acute myocardial infarction; AUROC: Area under the receiver operating characteristic curve; BCa: Bias-corrected and accelerated; CABG: Coronary artery bypass grafting; CAD: Coronary artery disease; CAG: Coronary angiography; CI: Confidence interval; ECG: Electrocardiogram; IQR: Interquartile range; LR: Likelihood ratio; NPV: Negative predictive value; NSTEMI: Non-ST-elevation myocardial infarction; PCI: Percutaneous coronary intervention; PPV: Positive predictive value; STEMI: ST-elevation myocardial infarction; TRIPOD+AI: Transparent Reporting of a multivariable prediction model for Individual Prognosis Or Diagnosis, updated for artificial intelligence

Acknowledgements

We would like to thank all individuals who participated in this study.

Authors' contributions

SJ, MC, and KHC conceived the study. YYL, YHJ, YN, SJ, MSS, and KHC designed the methodology. YYL, YHJ, and YN developed the software and performed the formal analysis. YHJ, YN, and HJA prepared the visualizations. SO, YWL, DYH, and MCK performed the investigation, validation, and data curation. KHL, DSS, YJH, JHK, and YA provided study resources. YA, MSS, and KHC supervised the study. MSS and KHC administered the project, and KHC acquired funding. YYL and MSS drafted the manuscript. All authors

reviewed and edited the manuscript. YYL and YHJ contributed equally to this work. All authors read and approved the final manuscript.

Funding

This research was supported by a grant from the Korea Health Technology R&D Project through the Korea Health Industry Development Institute (KHIDI), funded by the Ministry of Health & Welfare, Republic of Korea (grant number: RS-2024-00440410).

Availability of data and materials

The data used in this study are not publicly available because they contain potentially identifying patient information and are subject to privacy, legal, and institutional restrictions. The AI model and its source code are proprietary to VUNO Inc. and are not publicly available; however, the model architecture, training details, and operating points are fully described in Supplementary Material 3 (Supplementary Methods 1 and 2) to support reproducibility.

Declarations

Ethics approval and consent to participate

The present study received approval from the Institutional Review Board of Chonnam National University Hospital (IRB approval number: CNUH-2022-375). All participants provided written informed consent prior to enrollment. All procedures adhered to the principles outlined in the Declaration of Helsinki.

Consent for publication

Not applicable.

Competing interests

YHJ, YN, HJA, and SJ are employees of VUNO Inc. MC was an employee of VUNO Inc. The other authors declare that they have no competing interests.

References

1. Wu P, Yu S, Wang J, Zou S, Yao DS, Xiaochen Y. Global burden, trends, and inequalities of ischemic heart disease among young adults from 1990 to 2019: a population-based study. Front Cardiovasc Med. 2023;10:1274663. https://doi.org/10.3389/fcvm.2023.1274663.
2. Nowbar AN, Gitto M, Howard JP, Francis DP, Al-Lamee R. Mortality from ischemic heart disease. Circ Cardiovasc Qual Outcomes. 2019;12:e005375. https://doi.org/10.1161/CIRCOUTCOMES.118.005375.
3. Rao SV, O'Donoghue ML, Ruel M, Rab T, Tamis-Holland JE, Alexander JH, et al. 2025 ACC/AHA/ACEP/NAEMSP/SCAI guideline for the management of patients with acute coronary syndromes: a report of the American College of Cardiology/American Heart Association Joint Committee on Clinical Practice Guidelines. Circulation. 2025;151:e771–e862. https://doi.org/10.1161/CIR.0000000000001309.
4. Cho KH, Han X, Ahn JH, Hyun DY, Kim MC, Sim DS, et al. Long-term outcomes of patients with late presentation of ST-segment elevation myocardial infarction. J Am Coll Cardiol. 2021;77:1859–70. https://doi.org/10.1016/j.jacc.2021.02.041.
5. Khan R, Akhter J, Munir U, Almas T, Ullah W. Frequency of non-ST segment elevation myocardial infarction (NSTEMI) in acute coronary syndrome with normal electrocardiogram (ECG): insights from a cardiology hospital in Pakistan. Cureus. 2020;12:e8758. https://doi.org/10.7759/cureus.8758.
6. Chiu IM, Ouyang D. Acute myocardial infarction diagnosis: impact of artificial intelligence-powered ECG interpretation. Eur Heart J. 2025;46:1930–2. https://doi.org/10.1093/eurheartj/ehaf142.

7. Chen K-W, Wang Y-C, Liu M-H, Tsai B-Y, Wu M-Y, Hsieh P-H, et al. Artificial intelligence-assisted remote detection of ST-elevation myocardial infarction using a mini-12-lead electrocardiogram device in prehospital ambulance care. Front Cardiovasc Med. 2022;9:1001982. https://doi.org/10.3389/fcvm.2022.1001982.
8. Cho KH, Ji YH, Joo S, Chang M, Oh S, Lim Y, et al. Novel artificial intelligence model using electrocardiogram for detecting acute myocardial infarction needing revascularization. Eur Heart J Digit Health. 2025;6:608–18. https://doi.org/10.1093/ehjdh/ztaf049.
9. Martínez-Sellés M, Marina-Breysse M. Current and future use of artificial intelligence in electrocardiography. J Cardiovasc Dev Dis. 2023;10:175. https://doi.org/10.3390/jcdd10040175.
10. Attia ZI, Harmon DM, Behr ER, Friedman PA. Application of artificial intelligence to the electrocardiogram. Eur Heart J. 2021;42:4717–30. https://doi.org/10.1093/eurheartj/ehab649.
11. Mannhart D, Lischer M, Knecht S, du Fay de Lavallaz J, Strebel I, Serban T, et al. Clinical validation of 5 direct-to-consumer wearable smart devices to detect atrial fibrillation: BASEL wearable study. JACC Clin Electrophysiol. 2023;9:232–42. https://doi.org/10.1016/j.jacep.2022.09.011.
12. Sato M, Kodera S, Setoguchi N, Tanabe K, Kushida S, Kanda J, et al. Deep learning models for predicting left heart abnormalities from single-lead electrocardiogram for the development of wearable devices. Circ J. 2023;88:146–56. https://doi.org/10.1253/circj.CJ-23-0216.
13. Cho Y, Kwon JM, Kim KH, Medina-Inojosa JR, Jeon KH, Cho S, et al. Artificial intelligence algorithm for detecting myocardial infarction using six-lead

electrocardiography. Sci Rep. 2020;10:20495. https://doi.org/10.1038/s41598-020-77599-6.

14. Han C, Song Y, Lim HS, Tae Y, Jang JH, Lee BT, et al. Automated detection of acute myocardial infarction using asynchronous electrocardiogram signals-preview of implementing artificial intelligence with multichannel electrocardiographs obtained from smartwatches: retrospective study. J Med Internet Res. 2021;23:e31129. https://doi.org/10.2196/31129.

15. Gragnaniello M, Borghese A, Marrazzo VR, Maresca L, Breglio G, Irace A, et al. Real-time myocardial infarction detection approaches with a microcontroller-based edge-AI device. Sensors (Basel). 2024;24:828. https://doi.org/10.3390/s24030828.

16. Hasbullah S, Mohd Zahid MS, Mandala S. Detection of myocardial infarction using hybrid models of convolutional neural network and recurrent neural network. BioMedInformatics. 2023;3:478–92. https://doi.org/10.3390/biomedinformatics3020033.

17. Collins GS, Moons KGM, Dhiman P, Riley RD, Beam AL, Van Calster B, et al. TRIPOD+AI statement: updated guidance for reporting clinical prediction models that use regression or machine learning methods. BMJ. 2024;385:e078378. https://doi.org/10.1136/bmj-2023-078378.

18. Thygesen K, Alpert JS, Jaffe AS, Chaitman BR, Bax JJ, Morrow DA, et al. Fourth universal definition of myocardial infarction (2018). Eur Heart J. 2019;40:237–69. https://doi.org/10.1093/eurheartj/ehy462.

19. Byrne RA, Rossello X, Coughlan JJ, Barbato E, Berry C, Chieffo A, et al. 2023 ESC Guidelines for the management of acute coronary syndromes. Eur Heart J. 2023;44:3720–826. https://doi.org/10.1093/eurheartj/ehad191.

20. DeLong ER, DeLong DM, Clarke-Pearson DL. Comparing the areas under two or more correlated receiver operating characteristic curves: a nonparametric approach. Biometrics. 1988;44:837–45. https://doi.org/10.2307/2531595.
21. Wilson EB. Probable inference, the law of succession, and statistical inference. J Am Stat Assoc. 1927;22:209–12. https://doi.org/10.1080/01621459.1927.10502953.
22. Simel DL, Samsa GP, Matchar DB. Likelihood ratios with confidence: sample size estimation for diagnostic test studies. J Clin Epidemiol. 1991;44:763–70. https://doi.org/10.1016/0895-4356(91)90128-V.
23. Van Calster B, McLernon DJ, van Smeden M, Wynants L, Steyerberg EW. Calibration: the Achilles heel of predictive analytics. BMC Med. 2019;17:230. https://doi.org/10.1186/s12916-019-1466-7.
24. Steyerberg EW, Vickers AJ, Cook NR, Gerds T, Gonen M, Obuchowski N, et al. Assessing the performance of prediction models: a framework for traditional and novel measures. Epidemiology. 2010;21:128–38. https://doi.org/10.1097/EDE.0b013e3181c30fb2.
25. Efron B. Better bootstrap confidence intervals. J Am Stat Assoc. 1987;82:171–85. https://doi.org/10.1080/01621459.1987.10478410.
26. Austin PC, Steyerberg EW. Graphical assessment of internal and external calibration of logistic regression models by using loess smoothers. Stat Med. 2014;33:517–35. https://doi.org/10.1002/sim.5941.
27. Fleiss JL. Measuring nominal scale agreement among many raters. Psychol Bull. 1971;76:378–82. https://doi.org/10.1037/h0031619.
28. Cohen J. A coefficient of agreement for nominal scales. Educ Psychol Meas. 1960;20:37–46. https://doi.org/10.1177/001316446002000104.

29. Lee MS, Shin TG, Lee Y, Kim DH, Choi SH, Cho H, et al. Artificial intelligence applied to electrocardiogram to rule out acute myocardial infarction: the ROMIAE multicentre study. Eur Heart J. 2025;46:1917–29. https://doi.org/10.1093/eurheartj/ehaf004.
30. Gifft K, Ghadban R, Assefa N, Luebbering Z, Allaham H, Enezate T. The accuracy of distribution of non-ST elevation electrocardiographic changes in localising the culprit vessel in non-ST elevation myocardial infarction. Arch Med Sci Atheroscler Dis. 2020;5:226–9. https://doi.org/10.5114/amsad.2020.98924.
31. Huey BL, Beller GA, Kaiser DL, Gibson RS. A comprehensive analysis of myocardial infarction due to left circumflex artery occlusion: comparison with infarction due to right coronary artery and left anterior descending artery occlusion. J Am Coll Cardiol. 1988;12:1156–66. https://doi.org/10.1016/0735-1097(88)92594-6.
32. Kim SS, Choi HS, Jeong MH, Cho JG, Ahn YK, Kim JH, et al. Clinical outcomes of acute myocardial infarction with occluded left circumflex artery. J Cardiol. 2011;57:290–6. https://doi.org/10.1016/j.jjcc.2011.01.014.

Supplementary Information

Supplementary Material 1 (.docx). Study protocol. Protocol of the prospective study "Validation of portable ECG device among patients with coronary artery disease," including the sample size determination.

Supplementary Material 2 (.docx). TRIPOD+AI checklist.

Supplementary Material 3 (.docx). Supplementary methods, tables, and figures. Supplementary Methods 1 and 2 (model development and operating thresholds), Tables S1 and S2, and Fig. S1.

Supplementary Files

This is a list of supplementary files associated with this preprint. Click to download.

- 261023supplementarymaterial1studyprotocol.docx
- 261023supplementarymaterial2tripodaichecklist.docx